Letters on Materials 16 (1), 2026 pp. 84-91 www.lettersonmaterials.com

Received 15 November 2025; Accepted 12 January 2026
https://doi.org/10.48612/letters/2026-1-84-91 https://elibrary.ru/rislfw

Microstructural development in model and commercial Al-Cu based alloys during equal-channel angular pressing at elevated temperature
Part II. Comparison of grain refinement in the model Al-3%Cu alloy and the commercial AA2219 alloy

O. Sh. Sitdikov

sitdikov.oleg@imsp.ru

Institute for Metals Superplasticity Problems, Russian Academy of Sciences, Ufa 450001, Russia

Abstract: This study (Part II) quantitatively demonstrates the decisive role of thermally stable nanoscale dispersoids in accelerating grain refinement during equal-channel angular pressing of the commercial AA2219 Al-Cu alloy at 300°C, directly comparing it with the model Al-3%Cu alloy (see Part I). Through scanning electron microscopy with electron backscatter diffraction and transmission electron microscopy, it is shown that the AA2219 alloy achieves a substantially more refined and homogeneous ultrafine-grained structure after a cumulative strain of $e=12$, with an average grain size of ≈2.5 – 3.0 μm, a high-angle boundary fraction exceeding 55%, and an average misorientation of ≈24° and a volume fraction of new fine grains of ≈82%. These values significantly surpass those of the model alloy processed under identical conditions. The accelerated kinetics are attributed to a synergistic effect where fine, thermally stable dispersoids (e. g., aluminides of Zr, Mn, Cr) enhance strain localization via microshear band formation, suppress dynamic recovery by pinning dislocations and subboundaries, and stabilize the deformation-induced structure against static softening during inter-pass holdings. Thus, the introduction of dispersoids is proven to be a critical strategy for overcoming the limitations of dynamic recovery and achieving extensive grain refinement during high-temperature severe plastic deformation. The work establishes that dispersoids are crucial for tailoring a well-developed ultrafine-grained microstructure in commercial aluminum alloys under high-temperature severe plastic deformation conditions.

Keywords: AA2219 alloy, equal channel angular pressing, high temperature, microstructural evolution, grain refinement, continuous dynamic recrystallization, microshear bands, dispersoids

Acknowledgements: *The research was supported by the Ministry of Science and Higher Education of the Russian Federation within the framework of the state assignment of IMSP RAS. The author is grateful to Prof. T. Sakai (UEC Tokyo, Japan) for fruitful discussions that contributed to this study. Some experimental results were obtained in the joint research with I. A. Mazurina and I. S. Oleneva.*

1. Introduction

As established in the companion study (Part I), grain refinement in a model Al-3%Cu alloy during equal-channel angular pressing (ECAP) at 300°C occurs via continuous dynamic recrystallization (cDRX) initiated by the formation of microshear bands [1]. However, the efficiency of this process under high-temperature conditions is intrinsically limited by competing dynamic recovery, which impedes the accumulation of dislocations and the transformation of deformation-induced boundaries into high-angle grain boundaries. Consequently, the final microstructure of the model alloy remains only partially refined, retaining a significant fraction of low- and medium-angle boundaries even after substantial cumulative strain.

A primary pathway to overcome this limitation and achieve a uniform ultrafine-grained (UFG) structure under high-temperature severe plastic deformation (SPD) is through the strategic introduction of thermally stable, nanoscale dispersoids. These particles, typically formed by additions of transition metals such as Zr, Mn, and Cr, are known to pin grain boundaries and dislocations, thereby retaining the deformation-induced structure (the so-called "press-effect") and enhancing its thermal stability during subsequent annealing [2 – 9]. Hence, a considerable body of research has predominantly focused on and discussed their stabilizing role in the context of post-deformation heat treatment.

In contrast, this role during the deformation process itself, particularly in accelerating the kinetics of grain refinement, is less quantified [3, 6 – 9]. It remains unclear to what extent dispersoids can enhance the transformation rate of deformation-induced boundaries into high-angle grain boundaries during high-temperature SPD.

This study, presented as the second part of a comprehensive investigation, aims to bridge this gap by directly examining the accelerating effect of dispersoids on grain refinement. The commercial AA2219 Al-Cu alloy is employed, which contains a homogeneous dispersion of fine aluminides (e.g., Al_3Zr, $Al_{20}Cu_2Mn_3$) [10–13], and subject it to the same ECAP regime at 300°C as the model Al-3%Cu alloy in Part I [1]. The specific objectives are:

(i) quantitatively characterize the microstructural evolution and kinetics of grain refinement in the AA2219 alloy during high-temperature ECAP;

(ii) conduct a direct comparative analysis with the data from the model alloy (Part I), elucidating the decisive role of dispersoids;

(iii) discuss the underlying mechanisms by which dispersoids accelerate misorientation accumulation and promote the formation of a more fully developed UFG structure.

By this comparative approach, the intrinsic deformation processes were decoupled from the superimposed effects of dispersoids, providing a clear understanding of how these particles can be leveraged to tailor UFG microstructures in commercial aluminum alloys under high-temperature SPD conditions.

2. Materials and methods

The material used in this study was a commercial AA2219 alloy with a chemical composition of Al-6.4Cu-0.3Mn-0.18Cr-0.19Zr-0.06Fe (wt.%). To achieve a homogeneous microstructure and promote the precipitation of equilibrium phases, including fine aluminide dispersoids, the ingot was homogenized at 530°C for 6 hours, followed by furnace cooling. All procedures for ECAP processing, microstructural characterization, and quantitative EBSD analysis were identical to those described in detail for the model Al-3%Cu alloy in the companion paper (Part I) [1]. This includes the sample geometry, processing temperature (300°C), the same die (with $\Phi = 90°$, $\Psi = 0°$), pressing route (Route A), strain per pass ($\Delta e \approx 1$), strain rate ($\approx 3\ s^{-1}$), and the post-deformation cooling and inter-pass reheating protocol. The consistent application of these processing features ensures a direct and valid comparison of the microstructural evolution between the two alloys. For clarity in the present comparative analysis, it has been specified that the grain size values reported are based on the equivalent circle diameter of new grains delineated by high-angle boundaries ($\theta \geq 15°$) in EBSD data.

3. Results

3.1. Precipitate features in the commercial AA2219 alloy

Following homogenization, the commercial AA2219 alloy exhibited an equiaxed α-Al solid solution matrix with grain diameters ranging from 100 to 400 μm [10–12]. The microstructure contained several types of second phases (Fig. 1a), which are critical for its behavior during deformation. These included:

(i) larger precipitates of the main strengthening θ-phase (Al_2Cu), uniformly distributed within the grains and at boundary regions.

(ii) fine dispersoids, which remained thermally stable after annealing at 300°C (Fig. 1b). As established in prior studies of this particular alloy [10,12] and supported by independent literature [13], these dispersoids consist of plate-like T-phase ($Al_{20}Cu_2Mn_3$) particles up to 200 nm in length, and spherical precipitates of Al_7Cr (≈80 nm) and Al_3Zr (≈20 nm).

Notably, although the Al_3Zr phase may be partially coherent with the aluminum matrix, analysis in [10] indicated that approximately 80–90% of the dispersoids in the present alloy were incoherent. This incoherence renders them potent obstacles for dislocations and grain boundaries.

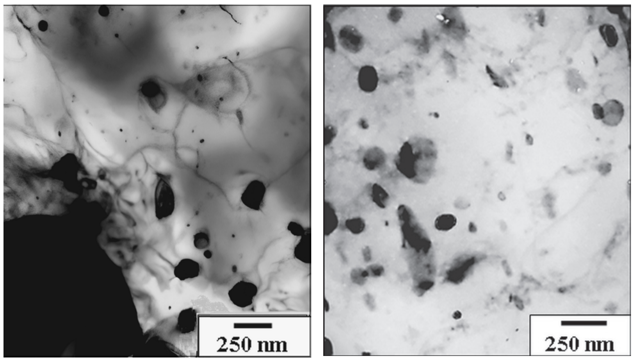

a b

Fig. 1. Typical TEM images of second-phase precipitates in the alloy AA2219: after homogenization (a); after homogenization and subsequent quenching from 300°C (b).

3.2. Microstructural evolution in the commercial AA2219 alloy

The microstructural response of the AA2219 alloy to ECAP at 300°C was markedly more complex and accelerated than that of the model Al-3%Cu alloy (see Part I [1]). Even at low strains ($e \leq 3$), the microstructure comprised a mixture of regions featuring a well-defined, uniform cellular/subgrain structure with prevalent low-angle boundaries (LABs) (Fig. 2a) alongside areas with a high density of intersecting deformation bands bounded by moderate-angle boundaries (MABs) and high-angle boundaries (HABs) (Fig. 2b).

This accelerated formation of deformation heterogeneities is directly attributed to the fine, homogeneous dispersion of the main secondary phase and dispersoids (Fig. 1), which promote strain localization at the mesoscale. While uniformly distributed nanoscale dispersoids in AA2219 ultimately promoted heterogeneous deformation, they can also contribute to homogenization of dislocation slip and suppress deformation banding in some regions, especially coherent dispersoids [14–16]. This homogenizing effect may be particularly significant in the earlier stages of plastic flow.

With increasing strain ($e = 6$ to 8), however, localized deformation became dominant, and extensive multiplication and intersection of deformation bands occurred, leading to the efficient fragmentation of the original coarse grains throughout the sample (Fig. 2c, d). The boundaries of these deformation features exhibited a rapid increase in misorientation.

By a strain of $e=12$, a nearly fully-developed ultrafine-grained (UFG) structure was established in the AA2219 alloy, with an average grain size of 2.5 – 3.0 μm (Fig. 2e, 3a, b). This structure was evidenced by almost continuous rings on the X-ray diffraction patterns (Fig. 3c). Figure 3a further presents misorientation distribution histograms for strains of $e=2$, 4, and 12, illustrating the progressive evolution of grain boundary character during ECAP. Quantitative analysis at $e=12$ showed a high fraction of high-angle boundaries ($f_{HABs}>55\%$) and an average misorientation angle (θ_{ave}) of ≈24°. The volume fraction of new fine grains reached ≈82% as measured by the point-counting method. These microstructural parameters significantly exceed those reported for the Al-3%Cu alloy [1].

TEM analysis confirmed the development of mutually intersecting deformation bands, which resulted in rectangular-shaped crystallites (Fig. 4). The critical role of dispersoids in this process was evident: at all strain levels, fine aluminides of Zr, Mn, and Cr were observed pinning dislocation and grain boundaries. This effective pinning retarded dynamic recovery and stabilized the deformation-induced boundaries, thereby facilitating the accumulation of dislocations and their subsequent transformation into HABs, as will be discussed below.

3.3. Boundary misorientation and grain refinement kinetics in the model and commercial alloys

A direct comparison of the misorientation parameters unequivocally highlights the influence of alloy composition on the grain refinement process (Figs. 5, 6). In the Al-3%Cu alloy, the average misorientation angle and HAB fraction increased gradually with strain, reaching ≈20° and ≈45% at $e=12$, respectively. The misorientation distribution remained broad, with significant proportions of LABs and MABs still present [1]. As discussed in Part I, this behavior is characteristic of a cDRX process, where grain refinement competes with dynamic recovery [8].

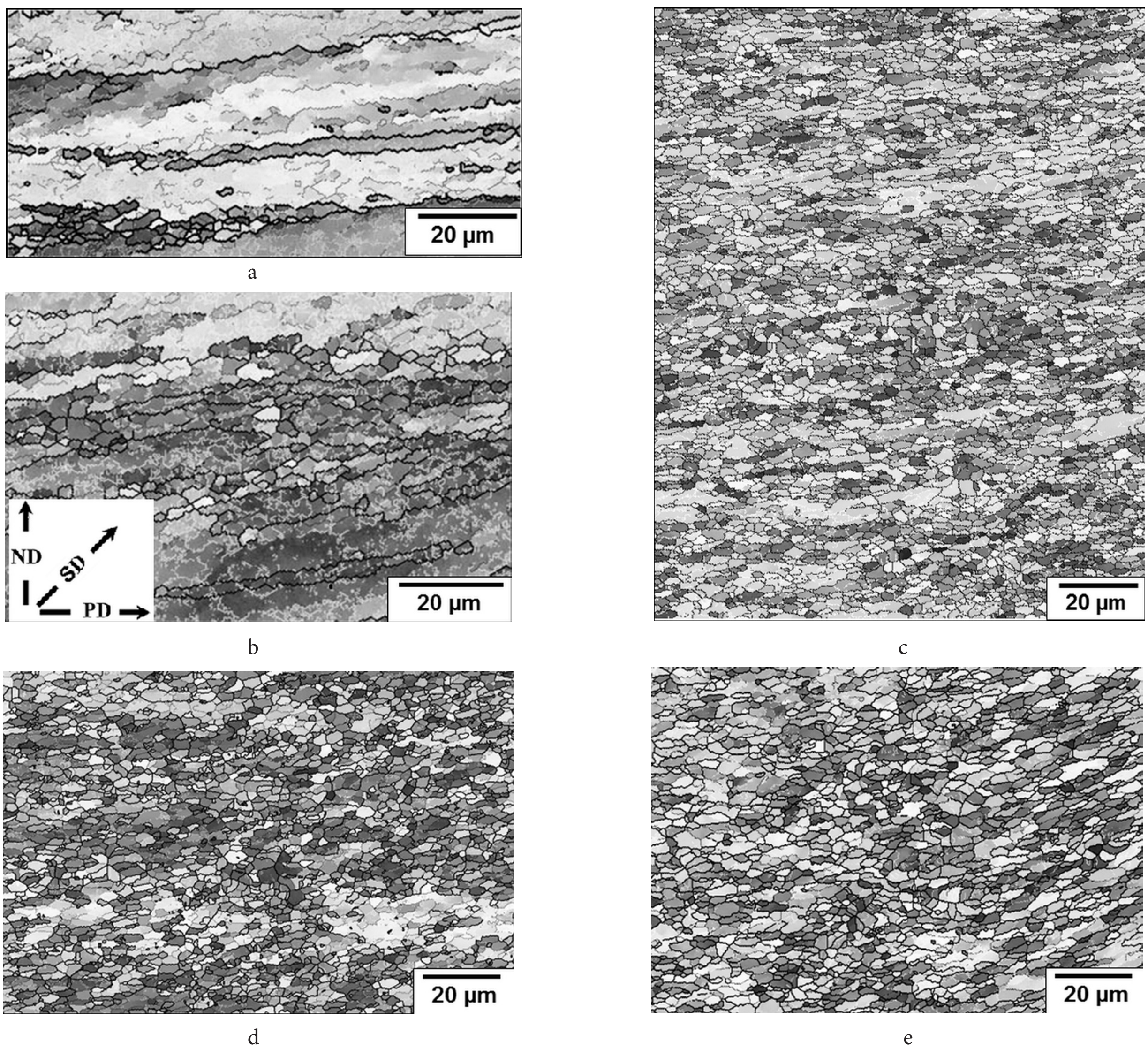

Fig. 2. Typical IPF-EBSD maps of the microstructure developed in the alloy AA2219 during ECAP at $T=300$°C to $e=3$ (a), $e=3$ (another area) (b), $e=6$ (c), $e=8$ (d), $e=12$ (e). Hereafter, PD denotes the pressing direction; ND is the normal direction; SD is the main shear direction in ECAP.

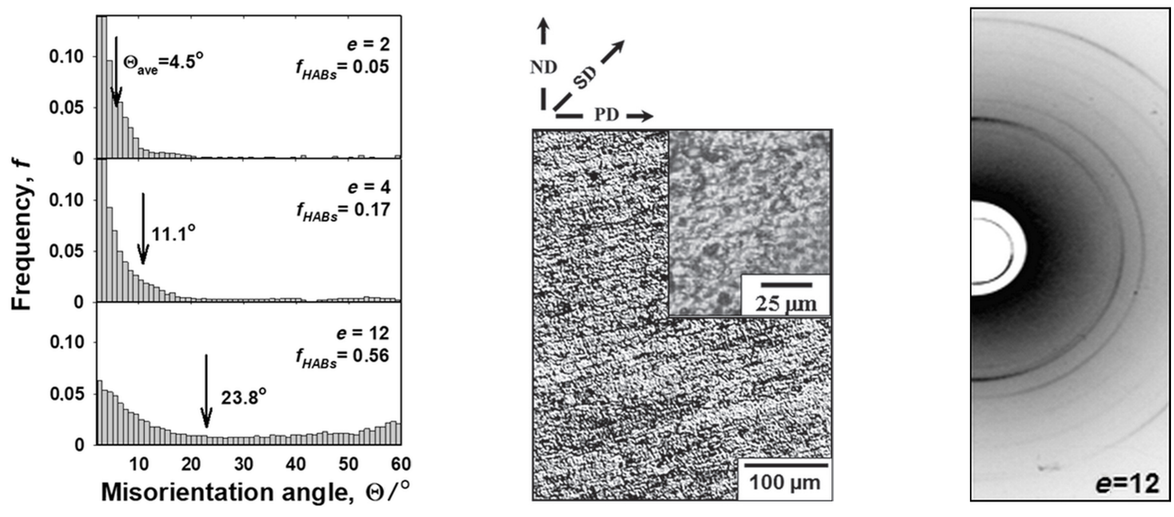

a b c

Fig. 3. Misorientation distributions of intercrystallite boundaries developed in the alloy AA2219 during ECAP at $T=300$°C (a), microstructure of the alloy AA2219 after ECAP at 300°C to $e=12$ optical microscopy (b), X-ray diffraction pattern after ECAP to $e=12$ (c).

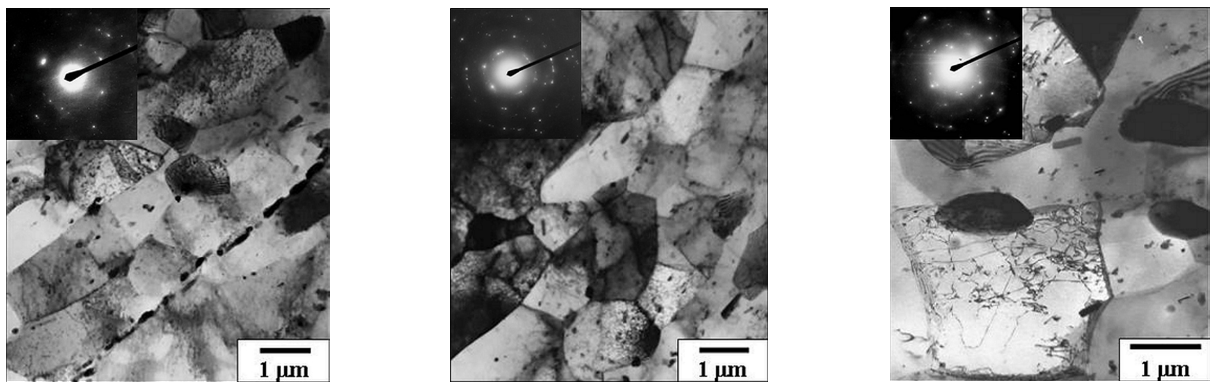

a b c

Fig. 4. Typical TEM images of the microstructure developed in alloy AA2219 after ECAP at 300°C to $e=3$ (a); $e=8$ (b) and $e=12$ (c). Selected area diffraction patterns were taken from the area with diameter 6 μm. Note the higher magnification applied in (c).

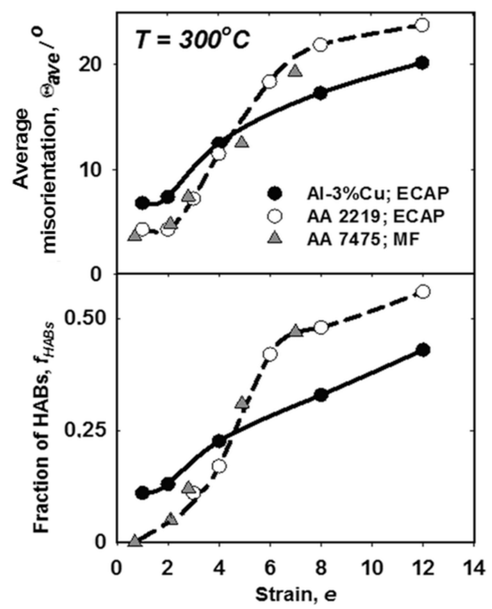

Fig. 5. Dependences of angular parameters of the structure formed during ECAP of the alloys Al-3%Cu and AA2219 on strain: average misorientation of intergranular boundaries (upper panel) and high-angle boundary (HAB) fraction (lower panel). Data for high-strength aluminum alloy AA7475 subjected to multidirectional forging (MF) at $T=300$°C [17] are represented for comparison.

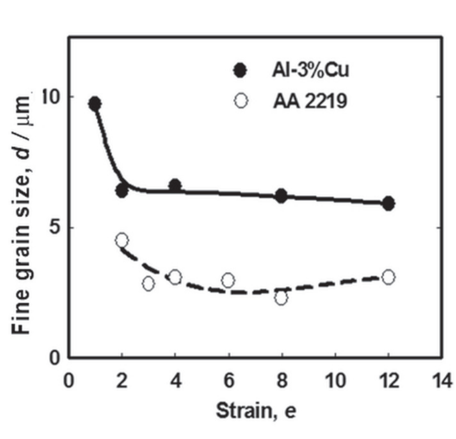

Fig. 6. Strain dependences of the sizes of new grains formed in the alloys Al-3%Cu and AA2219 during ECAP at $T=300$°C.

In stark contrast, the AA2219 alloy, although it showed some lower misorientation parameters at $e \le 4$, exhibited a much more rapid rise in both θ_{ave} and f_{HABs} during deformation to $e = 8$, after which the values tended to saturate near 25° and >60%. This kinetics of misorientation accumulation was quite similar to that of the high-strength commercial alloy AA7475 subjected to multidirectional forging at 300°C [17], whose data are included in Fig. 5 for reference. The similar structural evolution in both AA2219 and AA7475 underscores that this accelerated transition to high-angle boundaries is typical for alloys containing fine, thermally stable dispersoids.

The kinetics of grain refinement were also accelerated in AA2219, with the grain size stabilizing at a much smaller value (≈2.5 – 3.0 μm) compared to that of the Al-3%Cu alloy (≈6.0 μm) (Fig. 6).

4. Discussion

4.1. Comparative analysis of grain refinement kinetics and efficiency

A direct comparison of the microstructural parameters between the commercial AA2219 alloy (this work) and the model Al-3%Cu alloy (Part I) unequivocally highlights the decisive influence of alloy composition, specifically the presence of nanoscale dispersoids, on the grain refinement process during high-temperature ECAP.

The AA2219 alloy exhibited dramatically accelerated kinetics of misorientation accumulation and achieved a much more refined and homogeneous UFG structure. After a strain of $e = 12$ at 300°C, AA2219 developed a nearly fully developed UFG structure with an average grain size of ≈2.5 – 3.0 μm, a HAB fraction exceeding 55%, and an average misorientation of ≈24°. In stark contrast, the model Al-3%Cu alloy, processed under identical conditions, achieved only a partially refined microstructure with a coarser grain size, a lower HAB fraction, and a lower average misorientation of intercrystalline boundaries (Figs. 5, 6).

This superior refinement in AA2219 cannot be attributed to a different fundamental mechanism. As in the model alloy, grain refinement in the AA2219 occurs via cDRX driven by the formation and intersection of strain localization features, particularly microshear bands [11,12]. The critical difference lies in the kinetics and efficiency of this process, which are profoundly enhanced by the synergistic effect of the main strengthening θ-phase precipitates and, most importantly, the thermally stable nanoscale dispersoids (e.g., Al_3Zr, $Al_{20}Cu_2Mn_3$, Al_7Cr) present in AA2219.

4.2. The decisive role of dispersoids in microstructural evolution

Figure 7 shows typical examples of the interaction between deformation structures and secondary-phase particles in both alloys, which underpin the mechanisms responsible for the accelerated refinement in AA2219. Both the main strengthening phases and dispersoids serve several critical functions that collectively accelerate grain refinement in AA2219 compared to the Al-3%Cu alloy:

(i) enhanced strain localization and nucleation of new grains. The presence of non-shearable particles enhances strain localization during the deformation of aluminum alloys [e.g., 7,15,18,19]. A homogeneous distribution of these particles creates strong strain gradients at the mesoscale. For instance, non-shearable S-phase precipitates in AA2024-T8 were shown to generate a higher density of subboundaries and orientation gradients during rolling [18]. Similarly, research on an Al-Mg-Sc-Zr alloy demonstrated that non-shearable Al_3(Sc, Zr) dispersoids cause significant strain localization by interacting with dislocations [19]. In alloys containing such non-shearable precipitates, dislocations tend to distribute upon straining, resulting in higher stress fields [15]. Moreover, these particles increase the maximum attainable dislocation density during deformation by providing additional sites for dislocation storage, thus promoting the heterogeneous formation of a high density of microshear bands at lower strains. It is important to note, however, that a very high density of shearable, coherent dispersoids can, in contrast, homogenize slip and suppress deformation banding or delay the formation of dislocation boundaries [14,16]. In the present AA2219 alloy, however, the predominant dispersoids (e.g., Al_3Zr) are mostly non-coherent [10,12] and thus act as strong, localized obstacles, ensuring a net effect of enhanced strain localization, which is a key factor in the accelerated nucleation of new grains.

(ii) suppression of dynamic recovery. As confirmed by TEM analysis (Figs. 4, 7), the particles effectively pin dislocations and subboundaries. This pinning drastically restricts long-range dislocation rearrangement, thereby reducing the rate of dislocation annihilation and stabilizing the nascent boundaries [3, 7, 11, 20]. Consequently, this promotes faster accumulation of dislocations and facilitates the progressive transformation from low-angle to high-angle boundaries.

(iii) stabilization of deformation-induced grain boundaries. By retarding long-range boundary migration through Zener pinning [3, 7, 20], the particles stabilize the grain structure against significant growth, promoting the retention of the UFG structure even at high temperatures [7, 11, 20, 21]. This restriction of boundary mobility allows only short-range migration, which enables the new grains to attain a more equilibrium shape without losing the refined structure. However, even at a strain of $e = 12$, most fine grains retain a rectangular shape inherited from the microshear bands (Fig. 4 c), indicating the powerful pinning effect.

In contrast to AA2219, the model Al-3%Cu alloy lacks thermally stable dispersoids. Its θ-phase precipitates are the only ones present and are less effective at pinning dislocations and boundaries. Consequently, dynamic recovery occurs more readily, dislocation annihilation rates are higher, and boundary migration is less constrained. This limits the accumulation of misorientation, leading to a slower and less complete transformation of the deformation structure. The final microstructure is therefore coarser and contains a significant fraction of LABs and MABs even at high strains (see Part I [1]). Although the misorientation parameters were initially comparable or even somewhat higher in the Al-3%Cu alloy in the early stages of ECAP, this advantage was quickly lost at medium and high strains.

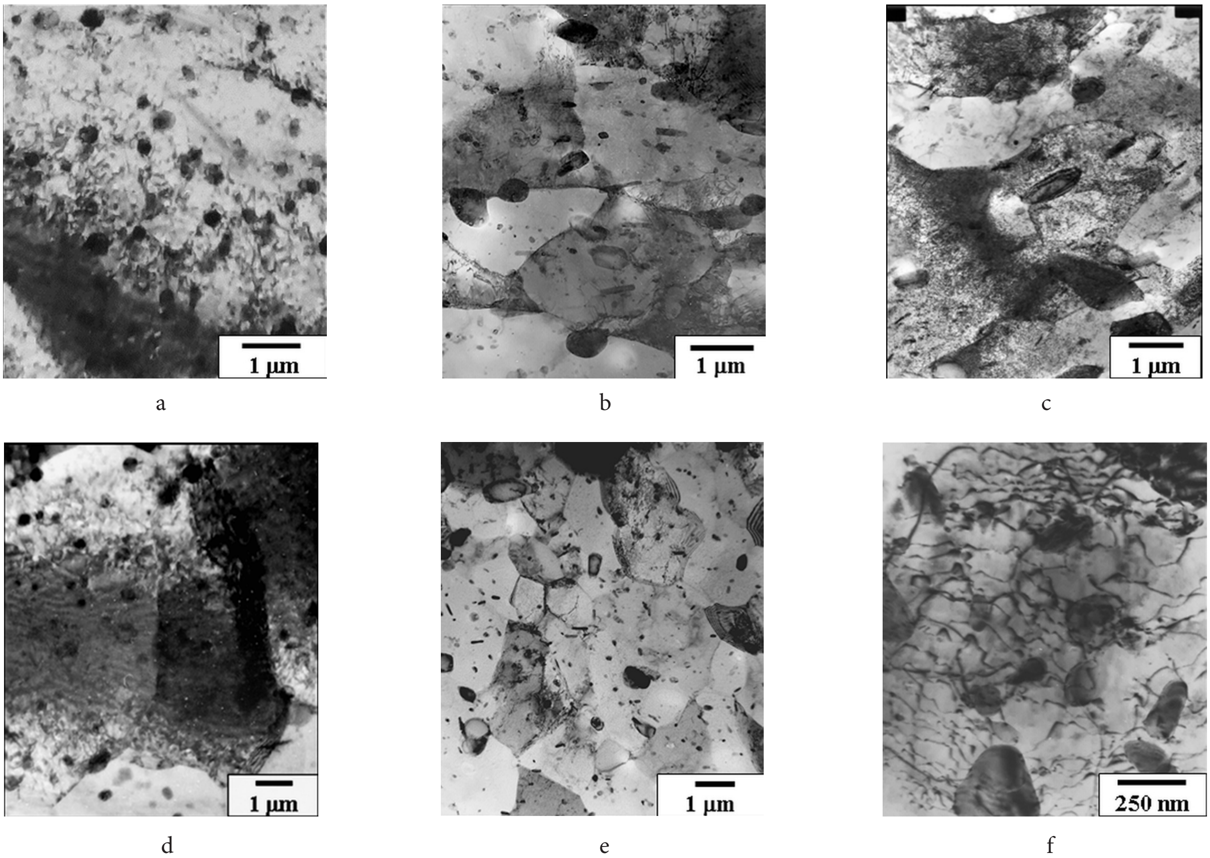

Fig. 7. Typical TEM images showing the interaction of dislocations with second-phase particles in the model Al-3%Cu alloy (a, d) and the commercial AA2219 alloy (b, c, e, f) after homogenization and subsequent ECAP to strains of $e=1$ (a, b), $e=2$ (c), and $e=4$ (d–f). The superior pinning of dislocations and subboundaries by the second phases is evident.

4.3. Competition between homogeneous and heterogeneous deformation at high temperature

The microstructural evolution during high-temperature ECAP is governed by a competition between two concurrent processes [8,11,12,22,23]:

(i) the formation of a relatively uniform, dynamically equilibrated subgrain structure within the interiors of many original grains, typical of hot deformation of aluminum alloys under high-rate dynamic recovery conditions.

(ii) the development of heterogeneous deformation/microshear bands, which become the dominant mechanism for grain refinement in the AA2219 alloy after a critical strain ($e \approx 2-3$).

The presence of dispersoids in alloys such as AA2219 or in AA7475 tilts this balance decisively in favor of heterogeneous deformation (Fig. 5). While they cannot completely suppress the formation of equilibrium subgrains in all regions, they ensure that strain localization via banding is both more prevalent and structurally significant. Acting as persistent structural elements, the stabilized boundaries of these bands thus become the primary sites for grain fragmentation and the nucleation of new HABs.

Although the high volume fraction of new grains (≈82%) confirms that dynamic refinement was extensive and dominated the microstructural evolution, an interesting finding of this study is the decrease in growth rate and the tendency of the misorientation parameters to saturate at high strains in the AA2219 alloy, while no such saturation is observed in the Al-3%Cu alloy. This saturation may indicate that even after high cumulative strains ($e=12$), the microstructure of AA2219 remains heterogeneous, consisting of a mixture of fine, recrystallized grains and larger, non-recrystallized fragments containing a subgrain structure (Fig. 2e,3), a state directly stabilized by the dispersoids impeding the development of a fully recrystallized microstructure. The saturation of misorientation parameters demonstrates that the heterogeneity in AA2219 may be significantly more pronounced and stable at high strains than in the model Al-3%Cu alloy.

This heterogeneity stems from the spatial variation in the effectiveness of deformation banding, which is critically influenced by the presence of a high density of thermally stable, incoherent dispersoids (like $Al_{20}Cu_2Mn_3$, Al_7Cr, Al_3Zr) in AA2219. These dispersoids effectively pin grain and subgrain boundaries, stabilizing the non-recrystallized regions and impeding their consumption by the new recrystallized grains [3,6,7,20]. Consequently, the potent Zener pinning exerted by these dispersoids not only explains the absence of a fully recrystallized structure but also results in a stable, heterogeneous microstructure, which is often desirable for achieving a favorable balance of strength and ductility.

4.4. Suppression of static softening processes during inter-pass holding

A significant challenge during high-temperature SPD with inter-pass holdings is the potential for static recovery and static recrystallization to erase the deformation structure and reduce the stored strain energy necessary for subsequent grain refinement [23, 24]. The present results demonstrate that the dispersoids in AA2219 are highly effective in mitigating this static softening.

As detailed in the Methods sections, the processing regime included water quenching after each pass and a 45-minute reheating to 300°C before the next operation. This inter-pass holding represents a substantial cumulative time at high temperature, creating ample opportunity for static restoration processes to occur. However, microstructural analysis reveals that the fraction of statically recrystallized grains remains low even in Al-3%Cu alloy (see Part I [1]). This effect is significantly more pronounced in the AA2219 alloy, where the potent Zener pinning effect exerted by the fine, thermally stable dispersoids (e. g., aluminides of Zr, Mn) further suppresses static softening. These particles effectively [3, 6, 7, 20]:

(i) pin dislocation substructures, slowing down their rearrangement and annihilation during the hold time.

(ii) anchor deformation-induced boundaries (including those of microshear bands), preventing their migration and growth that would be characteristic of static recrystallization.

By stabilizing the deformation-induced boundaries against static migration, the dispersoids ensure that the misorientation accumulated during the dynamic deformation phase is preserved and carried over to the next ECAP pass. This allows for the cumulative build-up of strain and misorientation over multiple passes, which is essential for the progressive transformation of subboundaries into high-angle grain boundaries via cDRX. In contrast, the model Al-3%Cu alloy (Part I), while also stabilized by θ-phase precipitates, is more susceptible to static softening due to the coarser nature and lower thermal stability of its secondary phases. Therefore, the dispersoids in AA2219 provide a critical advantage by offering synergistic stabilization during both the dynamic deformation and the static intervals, ensuring the overall dominance of the dynamic refinement pathway throughout the entire multi-pass processing cycle.

4.5. Outlook and ongoing research (announcement)

The present study quantitatively establishes the critical role of dispersoids in accelerating grain refinement during high-temperature ECAP up to e=12. The observed tendency for the microstructural parameters to saturate at high strains raises a fundamental question about the ultimate stability and refinement limits of such ultrafine-grained structures under continued severe deformation. In this context, preliminary results from ongoing research on the AA2219 alloy deformed under identical conditions to an exceptionally high cumulative strain of e=16 show a further stabilization of the microstructure. The grain size plateaus at ≈2.4 – 2.5 μm with a HAB fraction reaching 64 – 66%, confirming the saturation trend and underscoring the exceptional stability of the dispersoid-stabilized UFG structure. A detailed analysis of this stabilization phenomenon will be presented in forthcoming communications.

5. Conclusions

1. The presence of a homogeneous distribution of nanoscale dispersoids in the AA2219 alloy dramatically accelerates the kinetics of grain refinement during high-temperature ECAP compared to the model Al-3%Cu alloy (Part I).

2. After twelve ECAP passes (e=12), the AA2219 alloy achieves a more fully developed UFG structure with a grain size of ≈2.5 – 3.0 μm, a HAB fraction >55%, and an average misorientation of ≈25°, significantly surpassing the model alloy.

3. The accelerated refinement is attributed to the synergistic effect of the dispersoids, which promote strain localization (upon the prevalence of incoherent particles), suppress dynamic recovery, and stabilize deformation-induced boundaries through Zener pinning, thereby accelerating their transformation into high-angle boundaries.

4. Microstructural evolution involves competition between homogeneous subgrain formation and heterogeneous deformation banding, with dispersoids ensuring the dominance of the latter for effective grain refinement.

5. The dispersoids play a dual stabilizing role during high-temperature ECAP: they not only suppress dynamic recovery during deformation but also effectively prevent static softening during inter-pass holdings by stabilizing the dislocation structure and exerting Zener pinning. This ensures the cumulative accumulation of strain and misorientation over multiple ECAP passes, which is critical for the successful development of a UFG structure.

6. This study unequivocally demonstrates that dispersoids are the decisive drivers of microstructural evolution during high-temperature severe plastic deformation, crucial for tailoring high-quality UFG microstructures in commercial aluminum alloys.

References

1. O. S. Sitdikov, Microstructural development in the modeling and commercial Al-Cu based alloys during equal-channel angular pressing at elevated temperature. Part I. Microstructural evolution and continuous dynamic recrystallization in a model Al-3%Cu alloy, Lett. Mater. 15 (2025) 423 – 430. (companion paper)
2. N. P. Lyakishev (Ed.), Encyclopedic Dictionary of Metallurgy, Intermet Engineering, Moscow, 2000, 821 p. (in Russian)
3. F. J. Humphreys, M. Hatherly, Recrystallization and Related Annealing Phenomena, 2nd ed., Elsevier, Oxford, 2004.
4. I. S. Polkin, Structural hardening of titanium alloys, Tsvetnye Metally 11 (2010) 73 – 77. (in Russian)
5. O. G. Senatorova, V. V. Antipov, A. V. Bronz, A. V. Somov, N. Yu. Serebrennikova, High-strength and super high-strength conventional Al-Zn-Mg-Cu system-based alloys, their role in engineering and possibility of development, Tekhnologiya Legkikh Splavov 2 (2016) 58 – 72. (in Russian)
6. K. Edalati, A. Bachmaier, V. A. Beloshenko, Y. Beygelzimer, V. D. Blank, W. J. Botta, K. Bryła, J. Čížek, S. Divinski,

N. A. Enikeev, Y. Estrin, G. Faraji, R. B. Figueiredo, M. Fuji, T. Furuta, T. Grosdidier, J. Gubicza, A. Hohenwarter, Z. Horita, X. Zhu, Nanomaterials by severe plastic deformation: Review of historical developments and recent advances, Mater. Res. Lett. 10 (2022) 163 – 256.
7. T.-S. Liu, B.-X. Dong, H.-Y. Yang, F. Qiu, S.-L. Shu, Q.-C. Jiang, Review on role of intermetallic and ceramic particles in recrystallization driving force and microstructure of wrought Al alloys, J. Mater. Res. Technol. 27 (2023) 3374 – 3395.
8. R. Zhang, J.S. Zhang, W. Wang, Y.T. Tang, J. Jiang, R.C. Reed, J. Lin, Mechanistic insights and kinetics of continuous and geometric dynamic recrystallisation in hot deformed aluminium alloy, Acta Mater. 289 (2025) 120893.
9. M.V. Markushev, O.S. Sitdikov, E.V. Avtokratova, Nanostructuring, structure heterogeneity, and static strength of complex aluminum alloys, Phys. Mesomech. 28 (2025) 381 – 396.
10. R. Kaibyshev, O. Sitdikov, I. Mazurina, D.R. Lesuer, Deformation behavior of a 2219 Al alloy, Mater. Sci. Eng. A. 334 (2002) 104 – 113.
11. I. Mazurina, T. Sakai, H. Miura, O. Sitdikov, R. Kaibyshev, Effect of deformation temperature on microstructure evolution in aluminum alloy 2219 during hot ECAP, Mater. Sci. Eng. A 486 (2008) 662 – 671.
12. O. S. Sitdikov, Structural changes in a commercial Al-Cu alloy during hot equal channel angular pressing, Mater. Phys. Mech. 53 (2025) 89 – 108.
13. N. A. Belov, T. K. Akopyan, P. K. Shurkin, N. O. Korotkova, Comparative analysis of structure evolution and thermal stability of commercial AA2219 and model Al-2 wt%Mn-2wt%Cu cold rolled alloys, J. All. Comp. 864 (2021) 158823.
14. P.J. Apps, M. Berta, P.B. Prangnell, The effect of dispersoids on the grain refinement mechanisms during deformation of aluminium alloys to ultra-high strains, Acta Mater. 53 (2005) 499 – 511.
15. T.W. Jang, W.S. Choi, D.W. Kim, G. Choi, H. Jun, A. Ferrari, F. Körmann, P.-P. Choi, S.S. Sohn, Shear band-driven precipitate dispersion for ultrastrong ductile medium-entropy alloys, Nat. Commun. 12 (2021) 4703.
16. P. Thirathipviwat, T. Kotake, T. Suzuki, M. Hasegawa, K. Matsumoto, S. Sato, Effect of fine dispersoids on dislocation density and dislocation rearrangement of Al-Mn alloy during tensile deformation, Mater. Sci. Eng. A 927 (2025) 147997.
17. O. Sitdikov, T. Sakai, H. Miura, C. Hama, Temperature effect on fine-grained structure formation in high-strength Al alloy 7475 during hot severe deformation, Mater. Sci. Eng. A 516 (2009) 180 – 188.
18. D. Irmer, C. Yildirim, M. Sennour, V. A. Esin, C. Moussa, Effect of second-phase precipitates on deformation microstructure in AA2024 (Al-Cu-Mg): dislocation substructures and stored energy, J. Mater. Sci. 59 (2024) 18978 – 19002.
19. X. Chen, H. Chen, S. Ma, Y. Chen, J. Dai, Y. Brechet, G. Ji, S. Zhong, H. Wang, Z. Chen, Insights into flow stress and work hardening behaviors of a precipitation hardening AlMgScZr alloy: Experiments and modeling, Int. J. Plast. 172 (2024) 103852.
20. L. Cui, S. Shao, H. Wang, G. Zhang, Z. Zhao, C. Zhao, Recent advances in the equal channel angular pressing of metallic materials, Processes. 10 (2022) 2181.
21. O.S. Sitdikov, E.V. Avtokratova, S.V. Krymskyi, R.R. Ilyasov, M.V. Markushev, Effect of severe forging and rolling on the microstructure and mechanical properties of Al-Mg-Sc-Zr alloy, Inorg. Mater. 57 (2021) 101 – 111.
22. O.S. Sitdikov, E.V. Avtokratova, R.R. Zagitov, M.V. Markushev, Influence of the temperature of equal-channel angular pressing on fine-grain structure formation in the alloy Al-3%Cu, Lett. Mater. 11 (2021) 332 – 337. (in Russian)
23. O. Sitdikov, E. Avtokratova, M. Markushev, T. Sakai, Structural characterization of binary Al-Cu alloy processed by equal channel angular pressing at half of the melting point, Metall. Mater. Trans. A. 54 (2023) 505 – 525.
24. O. Sitdikov, E.V. Avtokratova, R.I. Babicheva, T. Sakai, K. Tsuzaki, Y. Watanabe, Influence of processing regimes on fine-grained microstructure development in an Al-Mg-Sc alloy by hot equal-channel angular pressing, Mater. Trans. 53 (2012) 56 – 62.